Declaration of Authorship

I, Gerardo Guillermo Cantón, declare that this thesis titled, 'Simulations of Synchrotron-Radiation Photon Distribution for the CERN Large Hadron Collider' and the work presented in it are my own. I confirm that:

- This work was done wholly or mainly while in candidature for a research degree at CINVESTAV.
- Where any part of this thesis has previously been submitted for a degree or any other qualification at CINVESTAV or any other institution, this has been clearly stated.
- Where I have consulted the published work of others, this is always clearly attributed.
- Where I have quoted from the work of others, the source is always given. With the exception of such quotations, this thesis is entirely my own work.
- I have acknowledged all main sources of help.
- Where the thesis is based on work done by myself jointly with others, I have made clear exactly what was done by others and what I have contributed myself.

Signed:

Date: August 2004

"God used beautiful mathematics in creating the world."

Paul Dirac

Abstract

Simulations of Synchrotron-Radiation Photon Distribution for the CERN Large Hadron Collider

by Gerardo Guillermo Cantón

At energies in the order of TeV, synchrotron radiation (SR) is very high, even in a hadron beam. SR could be regarded as an important heat load to the cryogenic system cooling the superconducting electromagnets. In this work SR is simulated using `Synrad3D` to analize which lattice elements of a section of the LHC absorb the most photon and analize how does it affect to have a sawtooth pattern in the beam screen.

Resumen

Simulations of Synchrotron-Radiation Photon Distribution for the CERN Large Hadron Collider

by Gerardo Guillermo Cantón

A energías en el orden de TeV la radición de sincrotrón es muy alta, incluso usando rayos de hadrones, esta radiación puede representar una carga calórica demasiado grande para electroimanes trabajando en estado criogénico. En este trabajo se simula la radiación de sincrotrón generada por un haz de protones en el LHC, utilizando `Synrad3D`, para analizar qué sección en un arco absorben la mayor cantidad de fotones y analizar como nos afecta tener en la pantalla ('beam screen') un patrón de diente de sierra.

Acknowledgements

I cannot express enough thanks to the members of this thesis committee: Dr. Rodrigo Huerta Quintanilla and Dr. Román Castro Rodriguez.

The completion of this project could not have been accomplished without the support of my supervisor, Jesus Guillermo Contreras Nuño; and so many people at CERN specially Frank Zimmermann.

I thank Consejo de Ciencia y Tecnología (CONACYT) and CINVESTAV for the financial support during my masters studies. I also thank CERN for all the information they make available to students such as myself.

I also want to thank the administrative personnel from CINVESTAV Mérida which has been helpful and efficient, specially Dr. Gerko Oskam and Zhirnay Rodriguez Pinelo.

Contents

List of Figures

List of Tables

Abbreviations

AFS	**A**ndrew **F**ile **S**ystem
ALICE	**A** **L**arge **I**on **C**ollider **E**xperiment
ATLAS	**A** **T**oroidal **L**HC **A**pparatu**S**
CERN	**C**onseil **E**uropéen pour la **R**echerche **N**ucléaire
	European Organization for Nuclear Research
CFH	**C**onfoederatio **H**elvetica **F**ranc
CMS	**C**ompact **M**uon **S**olenoid
FODO	**Fo**ocus/**D**ef**O**cus
LHC	**L**arge **H**adron **C**ollider
LHCb	**LHC** **b**eauty
LEP	**L**arge **E**lectron - **P**ositron Collider
LxPLUS	**L**x **P**ublic **L**ogin **S**ervice
SLC5	**S**cientific **L**inux **C**ERN **5**
SMIF	**S**ynrad3D **M**ain **I**nput **F**ile
SMOF	**S**ynrad3D **M**ain **O**utput **F**ile
SR	**S**ynchrotron **R**adiation
SSS	**S**hort **S**traight - **S**ection

Symbols

d	Distance	m
E	Energy	eV
P	Power	W (Js^{-1})
s	Transversal Direction	m
T	Temperature	K
γ_r	Relativistic gamma factor	
ε_c	Critical photon energy	eV
ρ	Radius	m
σ	Surface roughness	nm
ω_c	Critical photon frequency	rads^{-1}

Chapter 1

Introduction

In every circular particle accelerator, such as the LHC, energy is emitted in the form of synchrotron radiation (SR). This energy is then absorbed by the machine protection system. A circular accelerator consists mostly of 'superbends', electromagnets built with superconductor materials, which need to be very cold (around 4 K). If the LHC superbends heat up from 1.9 K to 4.5 K, the magnetic field strength decreases from 8.33 T to 6.8 T[1]. SR from bunches in the LHC creates electrons by photoelectric effect at the vacuum chamber wall. These electrons are accelerated by the positively charged particle bunch; when they impact the opposite wall, they can generate secondary electrons which can in turn be accelerated by the next bunch. Therefore, and avalanche production of secondary electrons gives rise to an electron cloud and its undesirable effects[2]. This is the reason why it is so important to know where and how SR is absorbed by each element of the lattice that conforms the accelerator.

At the LHC the maximum $\gamma_r = [1 - (\frac{v_r}{c})^2]^{-1/2}$ that can be reached depends on the maximum magnetic dipole field, which nominally is 8.33 T at 7 TeV beam energy, but the actual field limit depends on the heat load and temperature of the magnets and therefore on the amount of the radiation of the machine during operation[3]. So to achieve higher dipole fields we need to minimize the effects of SR.

It is not common that SR is considered as a problem in hadron storage rings, because it is very small compared to electron storage rings, but at very high energies such as the ones reached at the LHC it becomes a problem specially when it is then absorbed by the cryogenic system[3].

Work on this matter has been done by D. Sagan, G. Duncan, F. Zimmermann and G.H.I Maury[4]. In this thesis, we continue and extend the studies of [4]. These studies consist on the use of `Synrad3D` code, described in 4.1, to track SR photons at the LHC ring. Their simulations were performed for a 7 TeV proton beam energy and assumed a C layer of 10 nm on a Cu substrate. We study this problem in very particular conditions: at the LHC at CERN we focus on the main bending elements elements and we are adding the sawtooth pattern, a series of 30 μm high steps spaced at a distance of 500 μm in the longitudinal direction which is impressed on the horizontal outer side of the beam screen. Through simulation using the simulation software `Synrad3D`, we are able to tell which element absorb the largest number of photons and how many times did the photons bounce before being absorbed.

The main objective of this work is to analyze the difference in the simulation between using the sawtooth pattern or not in a small section of the main bending magnets with a 7 TeV proton energy beam.

Chapter 2

Fundamentals on Synchrotron Radiation

We call synchrotron radiation to the energy emitted by a charge which has a radial acceleration. It is produced in circular accelerators such as the LHC.

2.1 Radiation

The idea of electromagnetic waves has always fascinated the mind of physicists around the world. In 1887 G. Hertz generated, emitted and received electromagnetic waves. This was an experimental proof of Maxwell's equations. The source

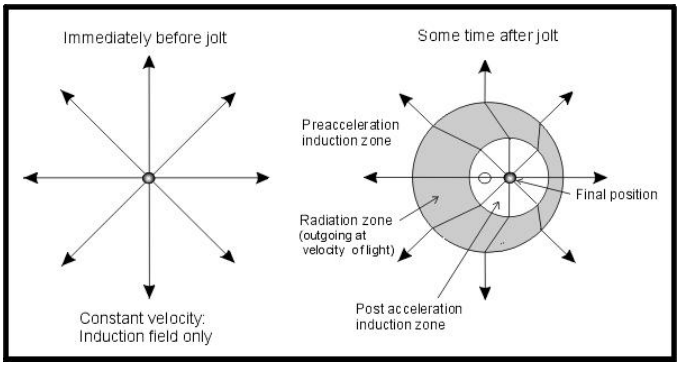

FIGURE 2.1: Electromagnetic field of a charge a) static b)after a short jolt
Picture taken from on [5]

of that radiation were oscillating charges.

First of all we should know that electromagnetic radiation is a consecuence of the finite velocity of light[6]. While a particle is at rest, or in a constant motion, it emits electric field lines radially out to infinity. If we suddenly accelerate this charge, the information of that acceleration travels with the speed of light, so that information is only known to the vicinity defined by:

$$\Delta d \leq c * \Delta t \tag{2.1}$$

The distortion of these lines, which is traveling away from the charge is what we call electromagnetic radiation. This concept is shown in Figure 2.1.

2.1.1 Conservation Laws

The emission of electromagnetic radiation from free electrons is a classical phenomenon. We may therefore use a visual approach to gain some insight into conditions and mechanisms of radiation emission. The emission of electromagnetic radiation involves two components, the electron and the radiation field. For the combined system energy–momentum conservation must be fulfilled. These conservation laws impose very specific selection rules on the kind of emission processes possible.

2.2 Synchrotron Radiation

The interest in electromagnetic theory grew in the mid 1940s with the development of the free electron radiation theories, mainly because of the development of circular high energy electron accelerators. In 1944 Pomeranchouk showed that there was a limit to the betatron principle, and that there was also an energy limit due to the losses from electromagnetic radiation. The energy that charged

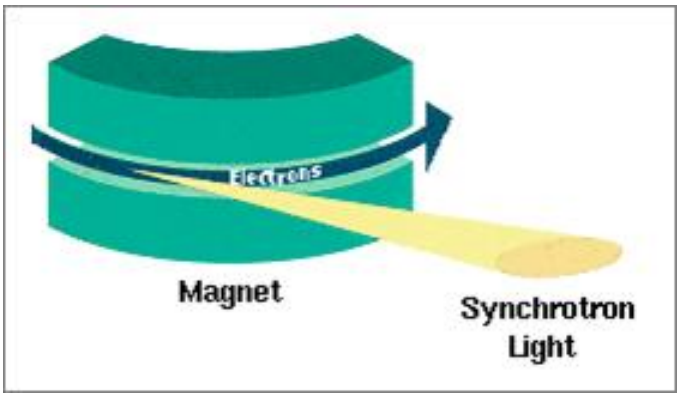

FIGURE 2.2: Synchrotron radiation produced by a bending magnet.
Picture taken from [7]

particles lose to SR posed technological and economic problems to increase circular accelerators maximum energy. To surpass this limitation, circular accelerators started growing diametrically[6].

When a relativistic beam of charged particles changes direction, it emits electromagnetic radiation, that can be seen as a search light, because it is highly collimated in the forward direction although it is broadband radiation, this is shown in Figure 2.2. The shortness of this pulse is what indicates the observer it has detected synchrotron radiation with a broadband spectrum which is characterized by the critical photon energy. This energy depends solely on the paticle's energy and its bending radius as shown in equation 2.2, where ε_c is the critical photon energy, ω_c is the critical photon frequency, E is the particle's energy, and ρ is the bending radius[6].

$$\varepsilon_c = \hbar\omega_c = \frac{3\hbar c}{2(mc^2)^3}\frac{E^3}{\rho} \tag{2.2}$$

There are particular characteristics of synchrotron radiation that depend on the magnetic devices used to generate that radiation, such as wigglers, undulators, wavelength shifters, etc. Nevertheless in this work we are only interested in bending magnets, furthermore superbends.

2.2.1 Superbends

When a charged particle enters a magnetic field region, the particle is deflected from its original trajectory perpendicularly to the magnetic field. The radius of this deflection depens only on the energy of the particle, its charge and the strength of the field. So we can express the critical photon energy as a function of the particle energy and the magnetic field. The numerical expression for an electron is shown in equation 2.3[6].

$$\varepsilon_c(keV) = 2.2183\frac{E^3(GeV^3)}{\rho(m)} = 0.66503E^2(GeV)B(T) \tag{2.3}$$

Where B is the strength of the field. Sometimes the critical energy required for a given experiment is too high to be reached using regular magnets, or if we have a fixed ρ and try to achieve maximum particle energy, as is the case of the LHC which had to fit in the LEP tunnel as mentioned in chapter 3. In those cases regular magnets are replaced with much stronger and shorter superconducting electromagnets. Conventional bending magnet fields rarely exceed 1.5 T, but superconducting magnets can be operated at 5 to 6 T or higher[6]

2.3 Radiation Power

To know the total radiated power we integrate the Poynting vector $\vec{S}$ over a closed surface that keeps the charge inside.

$$P = \oint \vec{S} \cdot d\vec{A} \tag{2.4}$$

Doing this we find that the power radiating from a charged particle moving perpendicularly to a magnetic field is proportional to the fourth power of the particle's momentum and inversely proportional to the square of the bending radius[6]. For that reason, a slight increase in energy for a high energy particle leads to a huge

increase of power loss due to synchrotron radiation. This is the reason why highest energy particle accelerators require a very large diameter.

Chapter 3

LHC

The Large Hadron Collider (LHC) at CERN is a wonder of engineering and technology. It lies inside a 26.7 Km circular tunnel and 100 meters under the ground. Its construction took over 15 years, involved engineers from all over the world and costed over 6.5 billion CHF. Inside the tunnel there are two counter-rotating hadron beams accelerated to energies up to 7 TeV each. This beams are then forced to collide inside four huge detectors that measures the products of the collision[8].

3.1 Characteristics

The 26,659 m tunnel used by the LHC was inherited from the LEP, when it was shut down. The basic layout consists of eight long straight sections and eight bending arcs[9]. In order to keep the 7 TeV proton beams in such a small orbit it was necessary to use 1,232 magnets with a 8.3 T field that extend to a length of 14.3 m each[3]. To achieve this, powerful magnetic field superconducting magnets were to be used. Because of commercial availability NbTi superconductors were used, this material needs to be cooled down below 4.2 K to reach the superconducting state. The solution was, and still is, to keep the magnets submerged in superfluid Helium below 2 K[9]. The basic layout is shown in Figure 3.1, where Beam 1 is

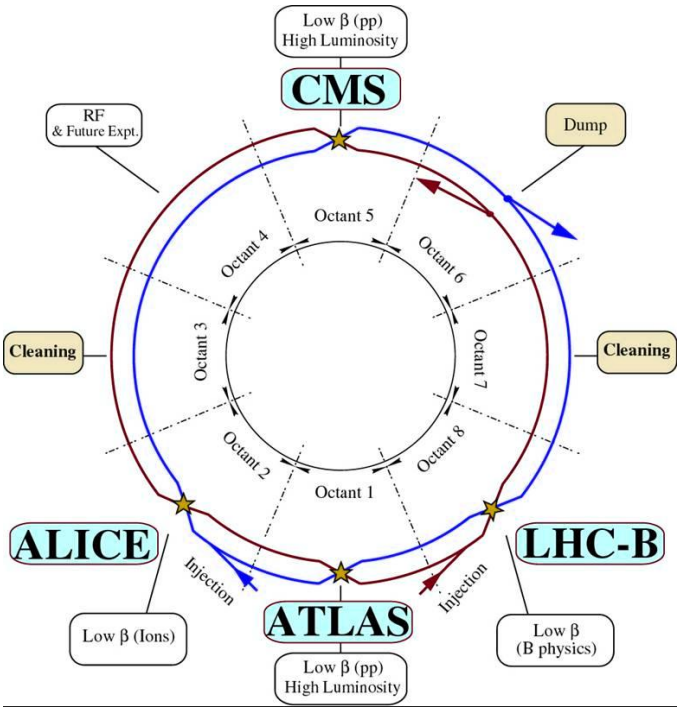

FIGURE 3.1: General schematic for the LHC
Picture courtesy of CERN.

shown in blue and circulates clockwise; and in red Beam 2 which rotates counter-clockwise. There are four intersections, one in each major experiment: ATLAS, CMS, LHC-b, and ALICE. The first two, ATLAS and CMS, are high luminosity experiments and are located diametrically opposite to each other, while LHC-b is an devoted to quark b experiments, and ALICE stands for A Large Ion Collider Experiment, which is self-explanatory and work with full stripped Pb ions. The LHC consist of 8 arcs and 8 straight section and it is divided in octants, that start at the center of on arc and end at the center of the next one[3]. The main parameters when working at its maximum energy are listed in Table 3.1.

3.1.1 Arc Cells

The arcs consist of 23 regular arc cells. These are made out of two 53.45 m long half cells each of which consist of one cold mass with a length of 5.355m (6.63 mlong cryostat) short straight section (SSS) assembly and three 14.3 m long dipole magnets. The optics of Beam 1 and Beam 2 are coupled by electrical connections

TABLE 3.1: Main parameters for proton-proton collisions

Energy	7 TeV
Dipole Field	8.33 T
coild aperture	56 mm
Luminosity	10^{34} s^{-1} cm^{-2}
Injection energy	450 GeV
Circulating current/beam	0.56 A
Bunch spacing	25 ns
Particles/bunch	1.1×10^{11}
Stored beam energy	350 MJ
Normalised trasverse emittance	3.75 μm
RMS bunch length	0.075 m
Beam lifetime	22 h
Luminosity lifetime	10 h
Energy loss/turn	6.7 keV
Critical photon energy	45 eV
Linear photon flux	1×10^{17} $m^{-1}s^{-1}$
Total radiated power/beam	3.8 kW

* This table was taken from "the LHC vacuum system", p. 292 [10].

of the main magnets. There is also a dispersion suppressor at every transition between arcs and straight sections. The arc cells emulate a FODO lattice[3].

3.1.2 Optics

The LHC optics design allows an optics matching with fixed and equal phase advances over the insertion regions for both beams that does not perturb the optics in the rest of the machine. The total number of particle trajectory oscillations during one revolution in the storage ring of the machine is adjusted by the optics of the arc cell. The flexibility of the phase advance over the insertions provides a measure for the flexibility of the total LHC optics and tell us how much liberty we have to change the phase advance between the main experimental insertions[3].

3.1.3 LHC Beam Pipe

Because of the high beam intensities given by luminosities such as the one shown in Table 3.1, the LHC cannot work the same way as the Tevatron, which uses a single vacuum chamber and one set of magnets for both beams, the LHC requieres a vacuum chamber and set of magnets for each beam, and the beams only share the regions where the collisions take place and are around 130 m long[3]. On one hand we have the price of the magnets and on the other hand we have the problem that there is not enough space in the LEP tunnel for two sets of magnets; as a result the LHC was built with twin bore magnets constructed of two sets of coils and beam channels within the same mechanical structure and cryostat[3].

90% of the LHC surface should be maintained below 20 K and is made of copper cladded stainless steel in order to reduce ohmic resistence. The rest can stay at room temperature and is made of thick copper beam pipe [3].

Another important feature of the beam pipe is the beam screen, this is a cooled screen intended to intercept SR at temperatures higher than 1.9 K and electrons due to electron clouds in order to prevent the magnets from heating. Figure 3.2 shows the conceptual design of the LHC beam screen[3][10]. The manufacturing process starts by co-laminating a specially developed low permeability 1mm thick austenitic stainless steel strip with a 75 μm copper sheet and rolling a saw-tooth structure which will intercept photons at normal incidence, thereby reducing the amount of reflected photons. The pumping slots are punched into this composite strip, which is then rolled into its final shape and closed by a longitudinal weld[10].

3.1.4 Cryogenics

The LHC uses cryomodules that consume liquid helium and expel evaporated helium. Each module looses 150 W statically in addition to the dynamic losses, that span from 100 W to 800 W. For operation at nominal field the pressure inside

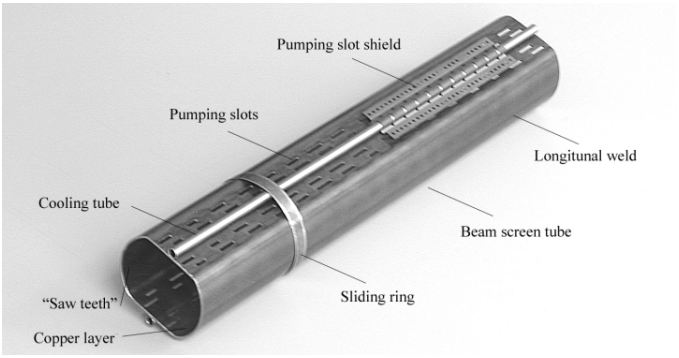

FIGURE 3.2: LHC Beam Screen
Picture courtesy of CERN.

TABLE 3.2: SR Parameters

Parameter	450 Mev	7 TeV
Total power/beam	0.066 W	3886 W
Energy loss per turn	0.11 eV	6.7 keV
average photon flux per metre and second	0.4×10^{16}	6.8×10^{16}
Photon critical energy	0.01 eV	43.13 eV
Longit. emittance damping time	5.5 yr	12.9 h
Trans. emittance damping time	11 yr	26 h

* This table was taken from the "LHC Design Report", p. 108 [3].

the helium tank has to be carefully controlled to avoid frequency variations of the cavity[3].

3.1.5 Synchrotron Radiation

The LHC is the first proton collider for which SR is a problem. At its highest energies SR gives rise to an important heat load to the beam screen[3], mentioned in 3.1.3. As shown in Table 3.2 each beam produce an average of 6.8×10^{16} photons per metre per second in the arcs, which corresponds to 3886 W. So the SR power per metre per bend per beam is 220 mW/m.

3.2 Electron Cloud Due to Beam Induced SR

When high energy SR photons strike a surface, they are able to set loose electrons out of the surface by ionizing it. This electrons are then attracted by the protons in the beam, they move, hitting the wall extracting even more electrons out of the wall, that will follow the next bunch of protons, this process leads to a fast building electron cloud, which is a very undesirable effect. The effects of electron clouds have been studied at CERN since 1997[11].

Chapter 4

Synrad3D

4.1 Introduction to Synrad3D

`Synrad3D` is a program built in Bmad. It was written by David Sagan using a photon scattering model developed by Gerry Dugan, both of them from Cornell University.

`Synrad3D` simulates the production and scattering of synchrotron radiation generated by an electron beam in a high energy machine. [12]. The `Synrad3D` program uses the Monte Carlo method for photon generation, scattering, and absorption calculations.

4.1.1 Physics of Synrad3D

This section is based on the Synrad3D user manual[12]

To generate photons, a section of the machine is selected. The user sets the total number of photons to be generated. `Synrad3D` calculates how many photons need to be generated within each machine element. The local bending field at the beam orbit is used to determine the photon spectrum.

Each photon is tracked from the point of origin to the point at which it hits the vacuum chamber wall. The angle of incidence relative to the local normal to the vacuum chamber is computed. The scattering probability is calculated, using this angle and the photon's energy. Using the value of this probability, the photon is either absorbed at this location, or scattered. If it is scattered, the scattering is taken to be elastic. That is, photon energy does not change. This ignores any florescence. Surface roughness, on the other hand is taken into account so there is a diffuse component to the scattering. Then the photon is tracked to the next hit on the vacuum chamber wall, and the probability of scattering is again computed. This process goes on until the photon is absorbed.

4.1.1.1 Photon Generation

Photon generation is based on the standard synchrotron radiation formulas, applicable for dipoles and quadrupoles. The radiation is assumed to be incoherent.

`Synrad3D` slices up each element longitudinally and generates photons from each slice. The number of photons generated in a slice weighted by the local probability of photon emission which depends on the local orbit curvature.

Photon generation is based upon the local field along the beam orbit. Thus, for example, particles in a bending magnet will radiate. The beam orbit is calculated from such things as the settings of steering elements, element misalignments, etc. as given in the lattice file. The beam orbit is the closed orbit.

When a photon is generated at a given longitudinal position, the beam's emittances and centroid are used so that the resulting photon distribution mirrors the Gaussian positional distribution of the beam. Horizontal/vertical coupling is taken into account in this calculation. The photon energy distribution will be the standard energy spectrum of photons generated in a bend.

A photon's initial angular orientation is generated by first using a random number generator to generate an angular orientation using a probability function that corresponds to the beam's angular distribution. The generated photons will have

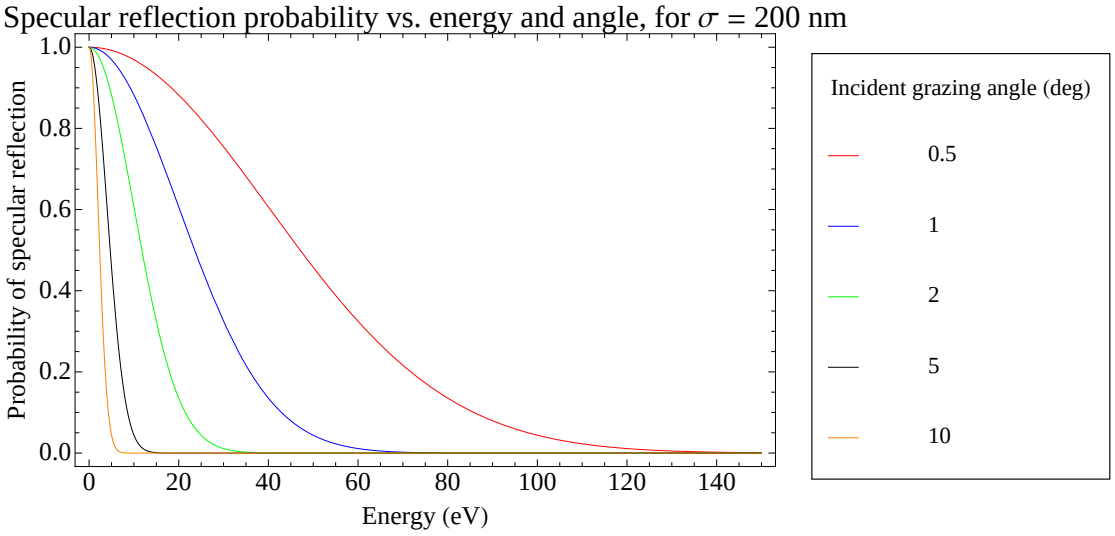

FIGURE 4.1: Specular reflection probability [13], vs. photon energy and angle, for an rms surface roughness of 200 nm.

the proper correlation between photon energy and photon angle. The plane of the bend may not be horizontal.

4.1.1.2 Photon Scattering

The probability that a photon will reflect specularly from a surface depends on the the rms surface roughness σ, the wavelength of the photon λ, and the grazing angle. As shown in equation 4.1: the formula for this probability is [13]

$$P_{\text{spec}} = \mathrm{e}^{-g(x,y)}, \tag{4.1}$$

where

$$g(x,y) = \frac{4\pi^2\sigma^2(x+y)^2}{\lambda^2} \tag{4.2}$$

where x is the cosine of the incident polar angle, and y is the cosine of the scattered polar angle.

For a typical technical vacuum chamber surface, the rms surface roughness $\sigma \gtrsim 200$ nm is greater than most of the X-ray wavelengths of interest. In this regime diffuse scattering from the surface dominates over specular reflection. This is illustrated in Fig. 4.1. The model for diffuse scattering used by `Synrad3D` assumes a Gaussian

distribution for both the surface height variations (rms σ) and for the transverse distribution.

The most general expression for the diffusely scattered power is complex, and involves an infinite sum. However, the expression simplifies substantially in the limit $g(x, y) \gg 1$. For very rough surfaces corresponding to technical vacuum chambers, for which typically $\sigma \gg \lambda$, this condition is satisfied over much of the region of interest.

4.1.2 Input Files

The input files used by `Synrad3D` are the following:

Synrad3D Main Input File (SMIF)

This file should be specified on the command line that invokes synrad3d, if it is not specified, it will select the default name "synrad3d.init". This file contains the parameters of the simulation

- The region where radiation is produced specified by the index numbers of elements in the lattice.
- The direction in which the photons are travelling when initially created.
- The minimun number of photons that need to be generated before `Synrad3D` will stop the simulation.
- the number of photons generated throughout the radiation production region.
- The minimun distance to track the particle beam between emission points.
- The particle beam size.
- The lattice file defining the optics of the accelerator.

- The wall file defining the vacuum chamber's geometry.
- The name of the output file.
- The surface roughness for the default surface.
- The surface roughness correlation for the default surface.
- The surface reflection file for non-default surface.
- The minimun and maximun initial energy values to be filtered by `Synrad3D`.

There are other parameters that can be specified in the SMIF, but are not mentioned here, because they are not relevant to this work.

Lattice File

This file cointains the complete description of the elements of the lattice, defining the optics of the machine. This file must be specified in the SMIF.

Vacuum Chamber Wall Definition file

The file specified in the SMIF defines the cross section of the vacuum chamber's wall at a number of longitudinal positions.

Chamber Surface Reflectivity file

The reflectivity of the vacuum chamber wall can be described on the surface reflection file specified in the SMIF. If no file is specified `Synrad3D` will use the default reflectivity, which is based on the refletivity of a Carbon film on Aluminum substrate.

4.1.3 Output Files

Synrad3d Main Output File

The name of this file must be specified in the SMIF. This file contains the information from the SMIF and the data generated for each photon. This information consists of:

- The number of the photon.
- The number of times the photon hit the wall.
- The photon energy.
- The position where the photon was generated.
- The position where the photon was absorbed.
- The distance traveled by the photon.
- The type of the lattice element where the photon was absorbed.

4.2 Tools

Given the nature of routines described in 4.1, using enough photons to obtain statistically valid results, running this program would take months in a regular commercial computer. To surpass this limitation the CERN *Lxplus* computing cluster was employed.

4.2.1 Lxplus

The Lx Public Login Service or Lxplus is a login service offered to all CERN users. This cluster consists in several public machines running SLC5 in 64 bit mode, where all interactive and batch systems are built on top of the CERN standart

Unix Enviroment. There is a wide range of shells available, that can be sorted in two groups: the C-shell like and the Bourne-shell like. We used Bash because of the full Linux based facilities. Since this machines are not to be used to store data a Workspace was made in the AFS file system that is accesible through normal system commands. Running CPU intense jobs in those machines is prohibited, so a system of jobs submissions to a set of queues with different limits on the available resources is at the disposal of the Lxplus user.

Chapter 5

Results

5.1 Simulation

We ran `Synrad3D` which was described in chapter 4. Our aim was to simulate 10^4 photons produced by a proton beam at 7 TeV energy. This amount of photons was used to balance a large enough number to present accurate statistical results and the amount of available computing time, but because of technical challenges mentioned in subsection 4.2.1, we divided the simulation into several simulations with a much smaller number of photons, there were simulations with 10, 20 and 50 photons each, which we can join together because photons do not interact with each other.

5.1.1 SMIF

The SMIF used to run this simulations used the following parameters:

- The wall file describing the vacuum chamber with a sawtooth pattern, of a series of 30 μm high steps at adistance of 500 μm in the longitudinal direction, which is on the horizontal. (sawtoohTEST.wall). The transversal section of the beam screen is shown in Figure 5.4.

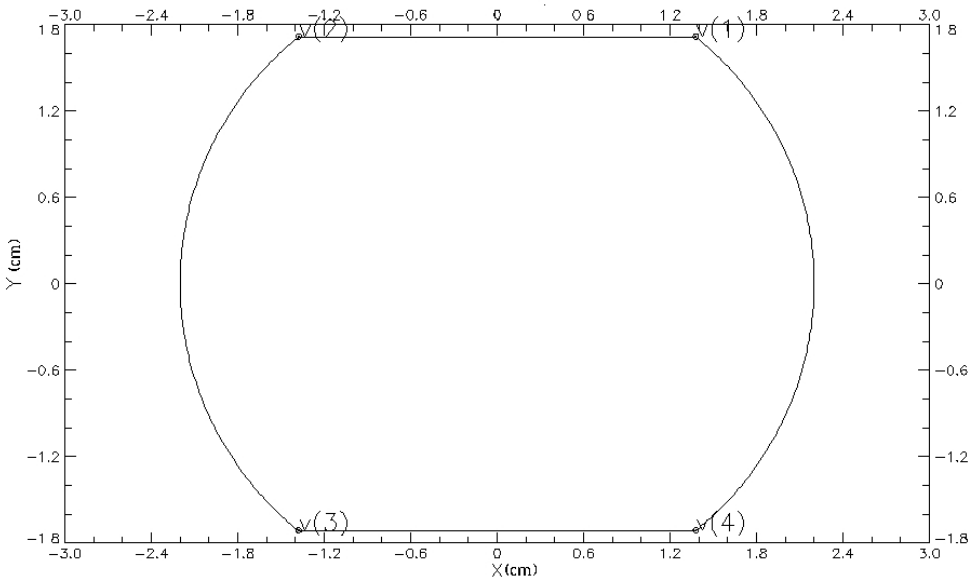

FIGURE 5.1: Transversal section of the beam screen in the cold arcs.
Image plotted with `Synrad3D`

- The lattice file which contains the version 6.5 of the LHC was employed. (V6.5.out.bmad)
- The starting element was set to be 142 and the ending element 146. All elements inside that range are bending dipoles.
- The photon direction was set to be positive wich means a forward generation.
- The number of photons varied between 10, 20 and 50.
- The seed for the random number generator was set to be the system clock.
- A custom reflectivity table was used. (reflectivity.table.C.CU.dat). This table assumes a carbon layer of 10 nm on a copper substrate. For this table the probability of reflection (P_{reflect}) was taken from the LBNL X-ray database[14].

5.1.2 SMOF

After all simulations were run through the batch system the results were concatenated into a single file containing a single table with the information of 9,227

photons that where generated, and absorbed by the beam screen between sections 142 and 146.

5.1.3 Secondary Simulation

In order to have data to compare to the data we obtained, we ran a single simulation featuring 10^4 photons using the same parameters except the sawtooth pattern of the wall file. In other words we simulated with the same parameters but with a smooth beam pipe. We kept the first 9,227 photons just to have the same number of photons in both simulations.

5.1.4 Analysis

In both simulations all photons were absorbed in the last element analyzed (bending magnet 146) with no rebounds. The exact position where photons were absorbed are shown in Figure 5.2. Figure 5.2 shows an histogram of photons absorbed versus the position on the s axis, The ones from the sawtooth pattern simulation is are shown in red, and the ones from the smooth surface simulation in blue.

The energies at which photons were absorbed are shown in Figure 5.3. It shows in blue the results for the primary simulation and in red the result for the secondary simulation. The mean energy from all photons absorbed by the sawtooth pattern is 27.109 eV and 27.113 for the smooth surface.

An histogram for the position X-Y where photons were absorbed are shown in Figure 5.4 for the main simulation and Figure 5.5 for the smooth beam pipe.

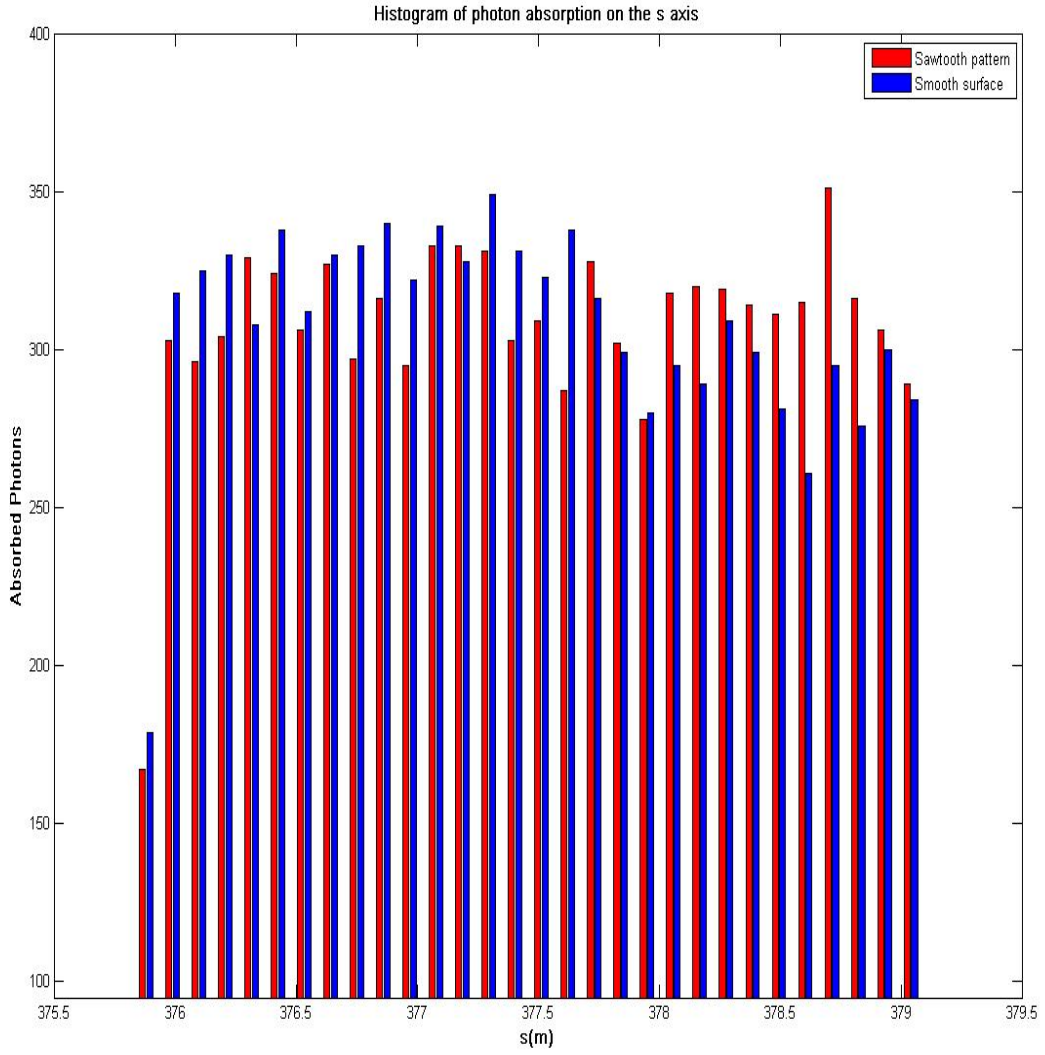

FIGURE 5.2: Position on the s axis where photons were absorbed.

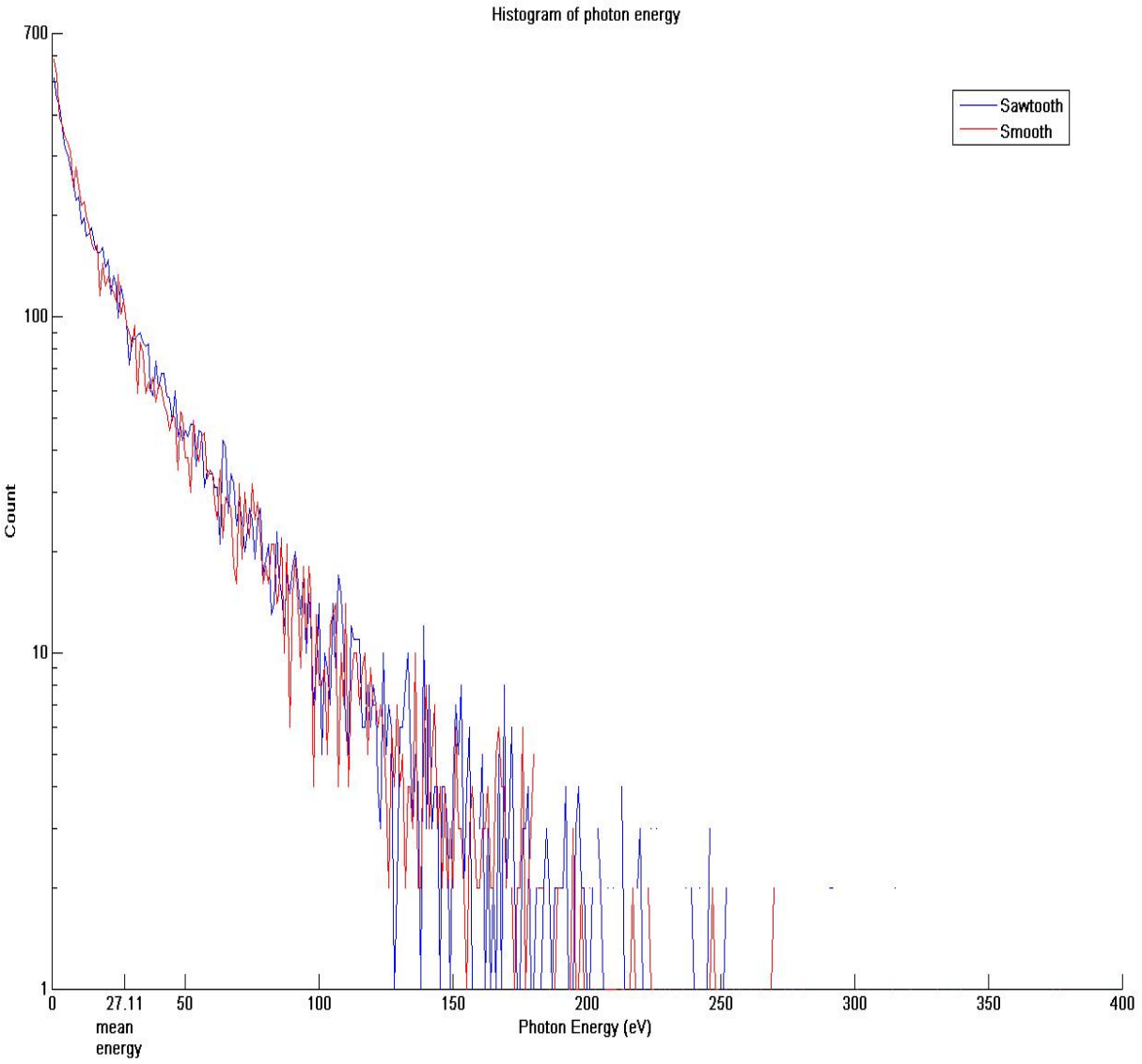

FIGURE 5.3: Energy of absorbed photons.

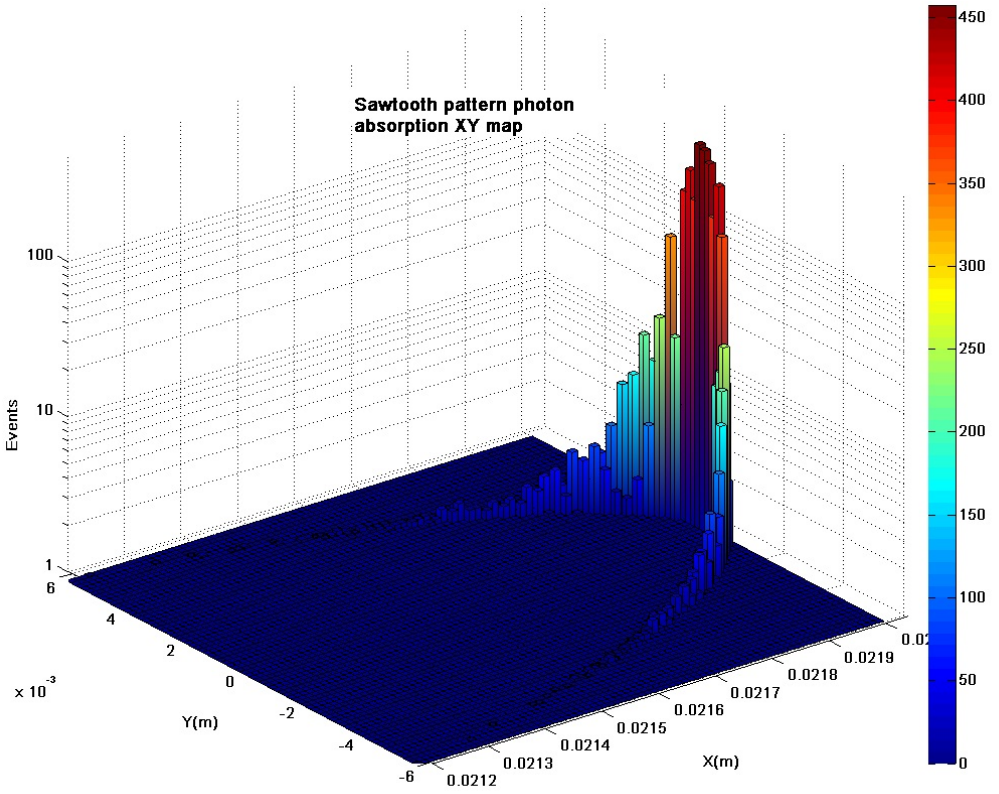

FIGURE 5.4: X-Y absorption points for the sawtooth pattern beam screen.

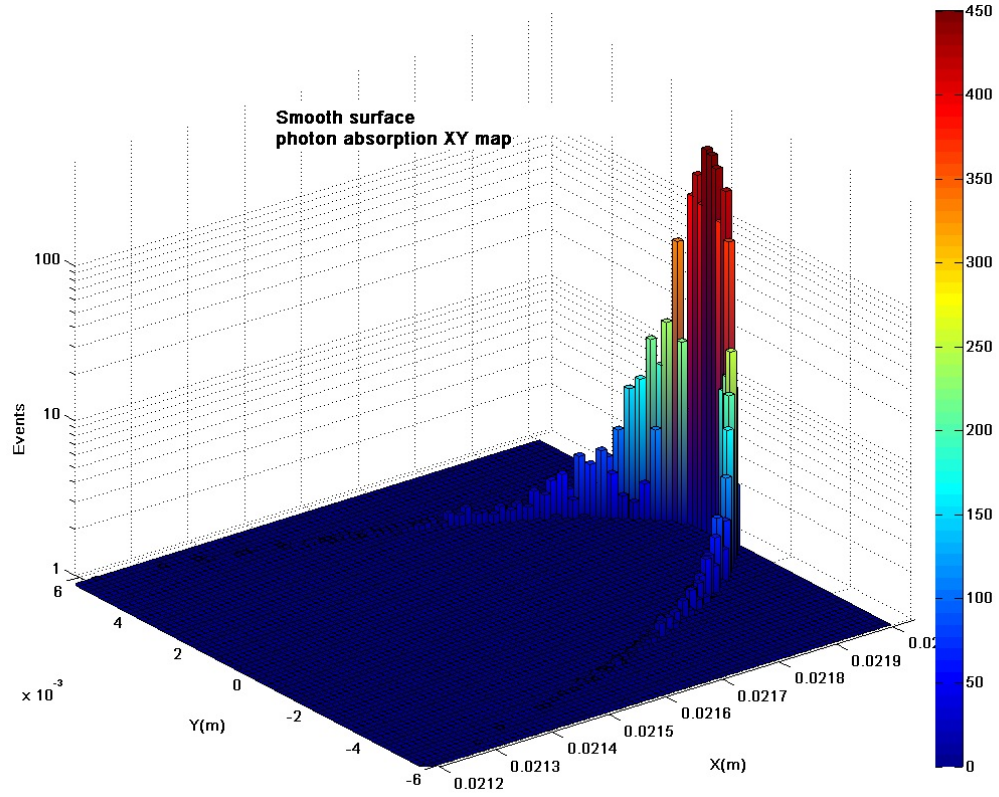

FIGURE 5.5: X-Y absorption points for the smooth surface beam screen.

Conclusion

No big difference between the Sawtooth Pattern beam screen and the smooth one were observed in both the position in the transversal direction (s) and energy of the absorbed photons (Figures 5.2−5.3). The difference that do appear, are only statistical error. I strongly believe this is because none of the photons bounced off the screen.

The simulation considering a sawtooth pattern in the beam screen showed a more extended distribution on the X-Y map Figure 5.4 than the one on smooth screen 5.5. This can make the cooling process more efficient.

Considering all this, the main conclusion is that the length we need to consider in our simulations should be longer than threee elements to really appreciate the difference the sawtooth pattern on the beam screen makes. But this simulation does help us to notice that in small accelerators having a sawtooth pattern on te beam screen would help us a little to nothing.

Future Work

The first step is to share our result with people at CERN, and compare with measurements. There are also two further steps that must be taken in the future to complete this work. The first one is to take an arc section long enough for photons to bounce at least two times in order to make the differences more noticeable. The second one is to take the whole arc into account, this will help us pinpoint the sections that suffer more heating due to synchrotron radiation and will help us

fully understand how the sawtooth pattern help us distributing the heat produced by SR and to reduce the primary emmision of electrons that would give rise to an electron cloud. And then back to sharing the resuts with CERN and comparing to measurements.

References

[1] FAQ CERN. LHC the guide, 2009. URL http://cds.cern.ch/record/1165534/files/CERN-Brochure-2009-003-Eng.pdf.

[2] M A Furman. Electron Cloud Effects in Accelerators. (arXiv:1310.1706):8 p, Oct 2013. Comments: 8 pages, contribution to the Joint INFN-CERN-EuCARD-AccNet Workshop on Electron-Cloud Effects: ECLOUD'12; 5-9 Jun 2012, La Biodola, Isola d'Elba, Italy.

[3] O. Brüning, P. Collier, P. Lebrun, S. Myers, R. Ostojic, J. Poole, and P. Proudlock. LHC design report(Volume I, The LHC main ring). *Reports-CERN*, 2004.

[4] H. Maury, D. Sagan, and F. Zimmermann. Synchrotron-radiation photon distributions for highest-energy circular colliders. *Proceedings of IPAC2013, Shanghai, China*, pages 1–3, December 2013. URL http://link.aip.org/link/?RSI/72/4477/1.

[5] URL http://physics.fullerton.edu/~jimw/general/inertia/efields.gif.

[6] H. Wiedemann. *Particle Accelerator Physics*. SpringerLink: Springer e-Books. Springer, 2007. ISBN 9783540490456. URL http://books.google.com.mx/books?id=S8CfmLe87RAC.

[7] URL http://upload.wikimedia.org/wikipedia/commons/5/58/Syncrotron.png.

[8] L.R. Evans. *The Large Hadron Collider: A Marvel of Technology*. Fundamental sciences. EPFL Press, 2009. ISBN 9782940222346. URL http://books.google.com.mx/books?id=tl8fLB1viQcC.

[9] Eberhard Keil. *The CERN Large Hadron Collider LHC*. 1996.

[10] O Grobner. The LHC vacuum system. In *Particle Accelerator Conference, 1997. Proceedings of the 1997*, volume 3, pages 3542–3546. IEEE, 1997.

[11] Giovanni Rumolo, J Esteban-Muller, G Arduini, T Pieloni, GHI Maury Cuna, W Höfle, C Zannini, W Venturini Delsolaro, V Kain, N Mounet, et al. Electron cloud observation in the LHC. Technical report, 2011. URL http://ab-abp-rlc.web.cern.ch/ab-abp-rlc-ecloud/LHC%20Papers%20&%20Talks/Electron_Cloud_Effects_in_the_LHC_Final_Report-Maury.pdf.

[12] D. Sagan G. Dugan. *Synrad3D Photon Tracking Program*. Cornell University, 2013. URL http://www.lepp.cornell.edu/~dcs/synrad3d.pdf.

[13] A.Spizzichino P. Beckmann. *The Scattering of Electromagnetic Waves from Rough Surfaces*. Pergamon Press, New York, 1963. ISBN 0890062382. URL http://www.amazon.com/Scattering-Electromagnetic-Surfaces-Artech-Library/dp/0890062382.

[14] URL http://henke.lbl.gov/optical_constants/layer2.html.